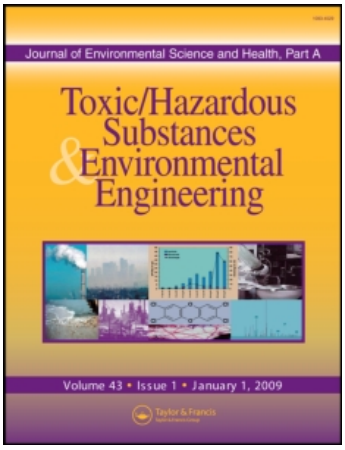

Journal of Environmental Science and Health, Part A
Publication details, including instructions for authors and subscription information:
http://www.informaworld.com/smpp/title~content=t713597268

Quantitative structure-activity relationship (QSAR) studies for predicting activation of the ryanodine receptor type 1 channel complex (RyR1) by polychlorinated biphenyl (PCB) congeners

Sierra Rayne [a]; Kaya Forest [b]
[a] Ecologica Research, Penticton, British Columbia, Canada [b] Department of Chemistry, Okanagan College, Penticton, British Columbia, Canada

Online publication date: 28 January 2010

To cite this Article Rayne, Sierra and Forest, Kaya(2010) 'Quantitative structure-activity relationship (QSAR) studies for predicting activation of the ryanodine receptor type 1 channel complex (RyR1) by polychlorinated biphenyl (PCB) congeners', Journal of Environmental Science and Health, Part A, 45: 3, 355 — 362
To link to this Article: DOI: 10.1080/10934520903467980
URL: http://dx.doi.org/10.1080/10934520903467980

Journal of Environmental Science and Health Part A (2010) **45**, 355–362

ISSN: 1093-4529 (Print); 1532-4117 (Online)
DOI: 10.1080/10934520903467980

Taylor & Francis
Taylor & Francis Group

Quantitative structure-activity relationship (QSAR) studies for predicting activation of the ryanodine receptor type 1 channel complex (RyR1) by polychlorinated biphenyl (PCB) congeners

SIERRA RAYNE[1] and KAYA FOREST[2]

[1]*Ecologica Research, Penticton, British Columbia, Canada*
[2]*Department of Chemistry, Okanagan College, Penticton, British Columbia, Canada*

A quantitative structure-activity relationship (QSAR) was developed to predict the congener specific ryanodine receptor type RyR1 activity of all 209 polychlorinated biphenyl (PCB) congeners. A three-variable QSAR equation was obtained via stepwise forward linear regression on an unsupervised forward selection reduced data set from an initial database. Application of the QSAR towards predicting EC_{2x} values for all 209 PCB congeners indicated good agreement in substitution pattern trends between the experimental and estimated data sets. The QSAR model predicts a less than two-fold increase in maximal potency among all congeners outside the experimental database, and it appears that no high-potency PCB congeners with EC_{2x} values much less than 0.2 μM exist. Increasing RyR1-neuro toxicity equivalents with increasing homologue number and Aroclor chlorination likely reflect indirect molecular controls on toxicity, since congeners with multiple ortho substituents—the primary structural feature controlling a lack of coplanarity and resulting neurotoxicity—are more likely to be found in higher homologues.

Keywords: Polychlorinated biphenyls (PCBs), quantitative structure-activity relationship, ryanodine receptor type 1 channel complex (RyR1), non-coplanar PCB toxicity, neurological disruption.

Introduction

Polychlorinated biphenyls (PCBs; Fig. 1) are ubiquitous environmental contaminants that occur in complex mixtures and display broad acting toxicity.[1] A number of studies over the past two decades have established that higher activities for a variety of PCB neurotoxicological mechanisms are associated with ortho substituted non-coplanar congeners.[2–9] These structural requirements indicate that PCB neurotoxicity occurs via different mechanisms than the known aryl hydrocarbon receptor (AhR) mediated dioxin-like toxicities, since these latter endpoints are enhanced by coplanarity.[10] In addition to these basic structural features for neurotoxicity, the influence of other chlorine substitution patterns on the biphenyl function appears to be important. For example, reduction of dopamine and catecholamine content in cells, [^{3}H] phorbol ester binding in cerebellar granule cells, and altered signal transduction (including calcium homeostasis and protein kinase C) by PCBs is enhanced by congeners with ortho/para or ortho/meta substitution.[2–4,11–27]

Since the mid-1990s, Pessah and coworkers have progressively developed a primarily qualitative structure-activity based understanding of how PCBs alter calcium regulation and associated neuronal signalling by ryanodine receptor (RyR) mediated mechanisms.[28–34] RyR receptors are proteins that act as high conductance calcium channels, and which release Ca^{2+} stored within sarcoplasmic/endoplasmic reticulum membranes.[34] The following three genetic isoforms of RyR receptors exist: RyR1, responsible for skeletal muscle excitation-contraction (E-C) coupling; RyR2, responsible for cardiac muscle E-C coupling; and RyR3, functioning in the central nervous system.[35–39] Studies conducted to date indicate that the PCB concentrations required to elicit RyR1 activity in vivo are within the ranges detected in organisms, including humans, following exposure to PCB sources.[40,41] These findings have increased interest in further studies regarding the RyR activity of both individual PCB congeners and their mixtures in the hopes of better defining the range of acute and chronic toxicities posed by these legacy contaminants. As part of the present work, we develop the first

Address correspondence to Kaya Forest, Department of Chemistry, Okanagan College; E-mail: kforest@okanagan.bc.ca
Received August 15, 2009.

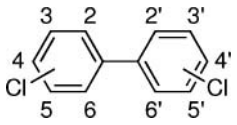

Fig. 1. General structure and chlorine substitution pattern numbering system for polychlorinated biphenyls (PCBs).

quantitative structure-activity relationship (QSAR) for predicting the RyR1 activity of all 209 PCB congeners. In addition, we apply the findings within a previously proposed neurotoxicity equivalence scheme in order to better understand what congener patterns and commercial mixtures are likely to pose the greatest RyR1 mediated neurotoxicity concerns.

Materials and methods

Experimental data on the potencies of the mono- through tetra-ortho substituted PCB congeners 4, 9, 18, 24, 26, 27, 30, 41, 49, 52, 66, 70, 75, 84, 95, 96, 101, 110, 111, 123, 126, 132, 136, 138, 149, 151, 153, 157, 159, 163, 170, 176, 180, 183, and 187 were obtained from ref.[42] PCBs 75, 111, 123, 126, 157, and 159 were excluded from QSAR development because one of their EC_{2x} (PCB congener concentration required to enhance specific [^{3}H]RyR1 binding by two-fold) or EC_{50} (PCB congener concentration required to enhance specific [^{3}H]RyR1 binding by half of maximum) activity endpoints could not be quantitated. EC_{2x} or EC_{50} values in concentration units of micromolar (μM) were converted to respective pEC_{2x} and pEC_{50} values by taking the negative logarithm of the experimental micromolar concentration data.

PCB molecular structures for all 209 congeners in SMILES[43,44] format were input to the E-DRAGON 1.0 software program (http://www.vcclab.org/lab/edragon/).[45,46] For each congener, 48 constitutional descriptors, 119 topological descriptors, 47 walk and path counts, 33 connectivity indices, 47 information indices, 96 two-dimensional autocorrelations, 107 edge adjacency indices, 64 Burden eigenvalues, 21 topological charge indices, 44 eigenvalue based indices, 41 Randic molecular profiles, 74 geometrical descriptors, 150 RDF descriptors, 160 three dimensional MoRSE descriptors, 99 WHIM descriptors, 197 GETAWAY descriptors, 154 functional group counts, 120 atom centered fragments, 14 charge descriptors, and 31 molecular properties were generated.

The SPARC software program (http://ibmlc2.chem.uga.edu/sparc/; August 2007 release w4.0.1219-s4.0.1219) was used to estimate octanol-water partitioning constants (log P) and octanol-water distribution constants (log D) for the training set compounds, as well as pK_a values for the phenolic groups of selected monohydroxy PCB congeners.[47,48] The three-dimensional geometries of the 29 PCB training set congeners were also gas phase energy minimized using the molecular mechanics MM2 method[49] and subsequently optimized in the gas and aqueous (COSMO[50] solvation model) phases using the semi-empirical PM6 method[51] in MOPAC 2009 (v. 9.045; http://openmopac.net/) with the following keywords in the input file header: gas phase (PM6 BONDS CHARGE = 0 SINGLET LET GNORM = 0 GRAPHF); aqueous phase (PM6 EPS = 78.4 RSOLV = 1.0 BONDS CHARGE = 0 SINGLET LET GNORM = 0 GRAPHF). The gas and aqueous phase PM6 calculations yielded the following three-dimensional molecular properties which were included in the QSAR development approach: standard state enthalpy of formation; total energy, electronic energy; core-core repulsion energy; Connolly molecular area (aqueous phase only); Connolly molecular volume (aqueous phase only); dipole; ionization potential; energies of the highest occupied molecular orbital (HOMO) and lowest unoccupied molecular orbital (LUMO) and the energy difference between the HOMO and LUMO; the biphenyl dihedral angle; partial Mulliken charges on all carbon atoms; and the most negative and most positive partial Mulliken charges on the corresponding chlorine substituents.

Unsupervised forward selection (UFS; http://www.vcclab.org/lab/ufs/start.html) was used to produce reduced descriptor data sets for both pEC_{2x} and pEC_{50} that contained maximal linearly independent sets of descriptor columns with a minimal amount of multiple correlation.[52] For pEC_{2x}, the UFS method produced a reduced descriptor data set containing the following variables (r-values against pEC_{2x} in parentheses): GATS6p ($r = 0.87$); BELe4 ($r = 0.83$); HATS6p ($r = -0.79$); Mor22p ($r = -0.76$); Mor16v ($r = 0.76$); Mor16p ($r = 0.76$); PM6 electronic energy ($r = 0.75$); RTe ($r = -0.75$); and BELm4 ($r = 0.75$). For pEC_{50}, the UFS method produced a reduced descriptor data set containing the following variables (r-values against pEC_{50} in parentheses): HATS5m ($r = 0.67$); RDF050m ($r = 0.64$); RDF065u ($r = -0.62$); BEHe5 ($r = 0.61$); R2e ($r = -0.59$); Mor15m ($r = -0.59$); BELm8 ($r = -0.57$); Mor25u ($r = -0.57$); and Mor13e ($r = -0.56$). Variable acronym definitions are available in the E-DRAGON for VCCLAB User Manual (http://michem.disat.unimib.it/chm/Help/edragon/index.html). Cluster analysis ($\alpha = 0.05$; standardized Euclidean measure; Ward clustering method)[53] and principle components analysis ($\alpha = 0.05$; scaling by correlation matrix) with KyPlot (v.2.b.15; Dr. K. Yoshioka, Tokyo Medical and Dental University, Tokyo, Japan) was also used to screen the variables for intercorrelation and confirm the suitability of the UFS reduced data sets. Stepwise forward multiple linear regression of the reduced data sets using F_{in}/F_{out} criteria of 0.2 and 0.1, respectively,[54] was conducted with KyPlot (v.2.b.15) against the experimental pEC_{2x} and pEC_{50} values to produce the final QSAR models.

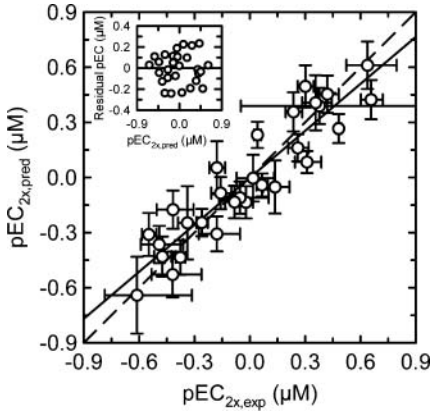

Fig. 2. Comparison between predicted (y-axis) and experimental (x-axis) pEC_{2x} values towards RyR1 activation using the QSAR regression equation given in the text. A 1:1 line (dashed) and a linear regression (solid) of the form $pEC_{2x,pred} = 0.85(\pm0.07)\times pEC_{2x,exp}\text{-}0.00(\pm0.02)$ ($r = 0.923$, $p_{m=0} < 10^{-12}$, $p_{b=0} = 0.95$) are shown. Inset shows a plot of residual $pEC_{2x,pred}$ prediction errors over the range of $pEC_{2x,pred}$ values.

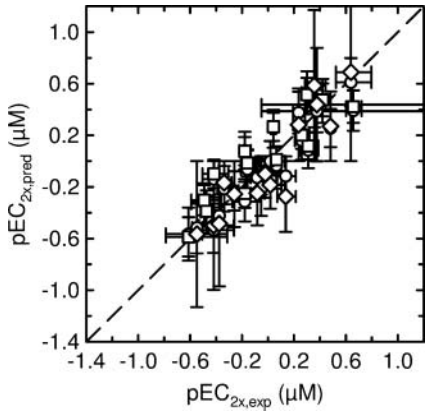

Fig. 3. Comparison between predicted (y-axis) and experimental (x-axis) pEC_{2x} values towards RyR1 activation during the leave-one-out (open circles) and two alternate divide-in-half (open squares and open diamonds, respectively) cross-validation exercises. A 1:1 line (dashed) is shown.

Results and discussion

Training of the pEC_{2x} QSAR model via stepwise forward linear regression of the UFS reduced data set gave the following three-variable predictive equation, $pEC_{2x}(\mu M) = 1.351\ (\pm0.579;\ \pm SE\ [standard\ error]) - 1.272\ (\pm0.374) \times GATS6p - 0.684\ (\pm0.256) \times Mor16p + 0.717\ (\pm0.274) \times HATS6p$, where GATS6p is the Geary autocorrelation lag 6 weighted by atomic polarizabilities, Mor16p is the 3D-MoRSE signal 16 weighted by atomic polarizabilities, and HATS6p is the leverage-weighted autocorrelation of lag 6 weighted by atomic polarizabilities (Fig. 2). Multicollinearity was not present among the final variables (Dillon and Goldstein condition number < 30) with the corresponding partial correlation matrix containing all r-values < |0.25| between the independent descriptors. The QSAR statistical quality of fit included an r-value of 0.923 ($r^2 = 0.852$; $r^2_{adj} = 0.835$), a standard error of 0.149, a coefficient of variation of −14.0, a predicted residual sum of squares of 0.742, an Akaike's information criterion of −22.4, and $p(F_{calc} = 55.5 > F_{0.05} = 3.0) < 10^{-9}$. No curvature was observed in the residuals plot (Fig. 2 inset; $p_{m=0} = 1$, $p_{b\neq0} = 1$). The variation inflation factor (VIF; $VIF = 1/(1\text{-}r^2)$, where r is the correlation coefficient of multiple regression between one independent variable and others in the equation; VIF = 1 indicates no self-correlation, 1< VIF < 5 is acceptable, and VIF > 10 indicates unstable regression[55]) was 3.1, indicating an acceptable level of self-correlation in the model.

The QSAR was limited to three independent variables ($2^3 = 8$), even though four ($2^4 = 16$) and possibly five ($2^5 = 32$) variables could have been used without exceeding overfitting criteria (2^N <n; where N is the number of independent variables and n is the size of training sample data set). Increasing the number of variables from three to four (Mor16v was the fourth chosen variable using stepwise regression) only improved the r^2 of the QSAR by 0.002 ($F_{in} = 0.32 > F_{in,crit} = 0.20$), compared to a Δr^2 of 0.059 for $N = 1 \rightarrow N = 2$ ($F_{in} = 8.6$) and a Δr^2 of 0.046 for $N = 2 \rightarrow N = 3$ ($F_{in} = 8.7$). In addition, the multicollinearity Dillon and Goldstein condition number exceeded 30 and the VIF was 162 with four variables, due to the high collinearity of the Mor16p and Mor16v descriptors. The pEC_{2x} QSAR model was validated using both the leave-one-out and N-fold (divide-in-half) cross-validation approaches for the training set compounds.[56] Good agreement was observed between the experimental and predicted pEC_{2x} values for all validation combinations, with low average signed and unsigned prediction errors, respectively, for the leave-one-out (0.00 and 0.12) and two alternate divide-in-half (0.06 and 0.15/-0.06 and 0.13) validations and a cross-validated r^2 value, q^2, of 0.805 and a q^2_{adj} of 0.802 (Fig. 3).

Attempts were made to develop a similar QSAR for predicting pEC_{50} values. The individual descriptor correlations with pEC_{50} were, in general, significantly less than the corresponding correlation with pEC_{2x}. Stepwise forward linear regression using the UFS reduced data set only resulted in QSARs with r^2 values of 0.60, 0.62, 0.65, and 0.66 for N = 3, 4, 5, and 6, respectively, indicating poor quality of fit and low potential for achieving a suitable r^2 value even by overfitting the model with $2^N >> n$. With N = 4, the following predictive equation was obtained, $pEC_{50}\ (\mu M) = -1.011\ (\pm0.501) + 0.043\ (\pm0.081) \times HATS5m + 0.164\ (\pm0.069) \times RDF050m - 0.331\ (\pm0.252) \times Mor15m - 0.036\ (\pm0.033) \times RDF065u$. The QSAR statistical quality of fit included an r-value of 0.789 ($r^2 = 0.623$; $r^2_{adj} = 0.559$), a standard error of 0.215, a coefficient of variation of −0.81, a predicted residual sum of squares of 1.85, an Akaike's information criterion of −0.24, and $p(F_{calc} = 9.9 > F_{0.05} = 2.8) < 10^{-4}$. No curvature was observed in the residuals plot ($p_{m=0} = 1$, $p_{b\neq0} = 1$). Multicollinearity was not present among the final variables according to the Dillon and Goldstein condition number (<30), with the

corresponding partial correlation matrix containing all r-values < |0.72| for the independent variables, but the VIF was 7.3, indicating an unacceptable level of self-correlation in the model. Regressing the predicted pEC_{50} against the experimental pEC_{50} for the training set gave a linear equation with a slope not equal to unity (0.62 ± 0.09) and a y-intercept not equal to zero (-0.10 ± 0.04) within the error range of the regression. Because of the poor predictivity of the pEC_{50} QSAR, and concerns regarding self-correlation in the model, it was not considered further and efforts were not undertaken towards predicting pEC_{50} values for PCB congeners outside the training set due to potential high unreliability of the estimates.

Application of the pEC_{2x} QSAR towards predicting EC_{2x} values for all 209 PCB congeners indicates good agreement in substitution pattern trends for the experimental and estimated data sets (Fig. 4). In the limited experimental data set, the most potent congeners were determined to be PCBs 95 ($EC_{2x} = 0.22 \pm 0.03$ μM) and 136 ($EC_{2x} = 0.23 \pm 0.07$ μM). The QSAR predicts that the following congeners will have RyR1 activation potencies equal to, or exceeding, the most potent congeners in the experimental data set (estimated EC_{2x} values [±SE of the regression estimate] in parentheses): 2,2′,3,5,6′-PCB 94 (0.24 ± 0.09 μM); 2,2′,3,3′,5,6′-PCB 135 (0.24 ± 0.09 μM); 2,2′,3,5,6,6′-PCB 152 (0.23 ± 0.09 μM); 2,2′,3,3′,5,5′,6-PCB 178 (0.22 ± 0.08 μM); 2,2′,3,3′,5,6,6′-PCB 179 (0.17 ± 0.07 μM); 2,2′,3,3′,4,5,6,6′-PCB 200 (0.24 ± 0.09 μM); 2,2′,3,3′,4,5′,6,6′-PCB 201 (0.24 ± 0.09 μM); 2,2′,3,3′,5,5′,6,6′-PCB 202 (0.12 ± 0.05 μM); 2,2′,3,3′,4,5,5′,6,6′-PCB 208 (0.18 ± 0.07 μM); and the fully chlorinated PCB 209 (0.27 ± 0.10 μM). As a result, the full congener QSAR model suggests that the experimental data set of Pessah et al.[42] adequately mapped the potential range of EC_{2x} values, since the QSAR model only predicts a less than two-fold increase in maximal potency among all congeners outside the experimental database. It appears that no high-potency PCB congeners with EC_{2x} values $<<0.2$ μM exist.

A review of the chlorine substitution patterns and pEC_{2x} values in the training set reported by Pessah et al.[42] suggests that, in addition to the likely minimum mono-ortho substitution (i.e., 2, 2′, 6, or 6′) required for activity, PCB congeners having only the 3,4,5- (or 3′,4′,5′-) positions substituted on at least one aryl moiety (and neither of the 2,6- or 2′,6′-positions substituted on the aryl moiety of interest), and either zero or one ortho substituent on the other aryl group, may be inactive (e.g., PCBs 123 [2,3′,4,4′,5′], 126 [3,3′,4,4′,5], and 157 [2,3,3′,4,4′,5′]). Conversely, if an ortho substituent is present on an aryl group with corresponding 3,4,5- or 3′,4′,5′-substitution, RyR1 activation is observed (e.g., PCBs 159 [2,3,3′,4,5,5′], $EC_{2x} = 1.95 \pm 0.41$ μM; 170 [2,2′,3,3′,4,4′,5], $EC_{2x} = 0.73 \pm 0.12$ μM; and 180 [2,2′,3,4,4′,5,5′], $EC_{2x} = 0.96 \pm 0.22$ μM). This structural pattern was also observed for PCB mediated effects on cytotoxicity, calcium homeostasis, inositol phosphates, protein kinase C translocation,[2–5,13,21,23] and previous RyR activity studies by Pessah and coworkers.[28,31,32] Pessah et al.[42] also reported that the 2,4,4′,6-substituted PCB 75 was inactive, and rationalized this finding as di-para substituted PCBs being generally less active towards RyR1. However, the presence of another 2,4,4′,6-substituted congener (2,2′,3,4,4′,5′,6-PCB 183) in the training set that is

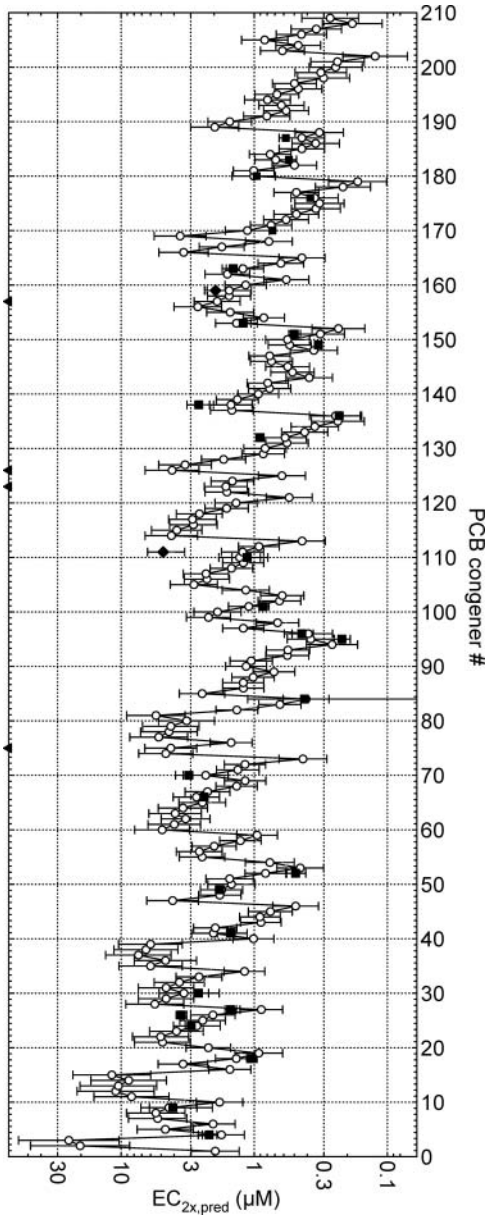

Fig. 4. Estimated pEC_{2x} values towards RyR1 activation for all 209 PCB congeners using the QSAR regression equation given in the text (open circles), along with corresponding experimental pEC_{2x} values (from ref. [42]) for congeners used in the QSAR training set (filled squares). Error bars represent standard errors about the QSAR model estimates. Two PCB congeners with experimental pEC_{2x} values (from ref. [42]), but which were not used in the training set due to an absence of measurable pEC_{50} values (PCBs 111 and 159), are also shown (filled diamonds). The four PCB congeners with inactivity in both pEC_{2x} and pEC_{50} experimental reporting (PCBs 75, 123, 126, and 157; ref. [42]) are shown with filled up triangles at the upper limit of the y-axis.

Table 1. PCB congeners expected to be inactive toward activation of RyR1 based on the presence of a 3,4,5- or 3′,4′,5′-chlorine substitution pattern with no adjacent ortho (2,6- or 2′,6′-) chlorine substituents and non- or mono-ortho substitution on the other aryl group.

Congener #	*Chlorine substitution*	*Experimental $EC_{2x}(\mu M)$*	*Predicted $EC_{2x}(\mu M)$*
38	3,4,5-	n/t[a]	6.5 (3.8 to 11.3)
76	2,3′,4′,5′-	n/t	1.5 (1.0 to 2.1)
78	3,3′,4,5-	n/t	4.2 (2.6 to 6.9)
81	3,4,4′,5-	n/t	5.5 (3.3 to 9.1)
122	2,3,3′,4′,5′-	n/t	1.6 (1.1 to 2.3)
123	2,3′,4,4′,5′	inactive[b]	1.6 (1.1 to 2.4)
124	2,3′,4′,5,5′-	n/t	1.5 (1.0 to 2.1)
126	3,3′,4,4′,5	inactive[b]	4.1 (2.6 to 6.6)
127	3,3′,4,5,5′-	n/t	3.3 (2.1 to 5.2)
157	2,3,3′,4,4′,5′	inactive[b]	1.9 (1.3 to 2.8)
162	2,3,3′,4′,5,5′-	n/t	1.6 (1.1 to 2.3)
167	2,3′,4,4′,5,5′-	n/t	1.8 (1.2 to 2.6)
169	3,3′,4,4′,5,5′-	n/t	3.6 (2.3 to 5.6)
189	2,3,3′,4,4′,5,5′-	n/t	2.0 (1.3 to 3.0)

Estimated EC_{2x} potencies (standard error range in parentheses) from application of the QSAR model described in the text are also given. [a]not tested. [b]from ref. [42].

comparatively active ($EC_{2x} = 0.55 \pm 0.07$ μM) relative to many other training set congeners precludes a general assessment regarding the potential deactivating potential of a 2,4,4′,6-substitution pattern.

Assuming that at least mono-ortho substitution is required for measurable RyR1 activity, and that a solely 3,4,5- or 3′,4′,5′-substituted aryl moiety with only zero or one ortho chlorine on the other aryl function may deactivate RyR1 activity, the group of PCB congeners shown in Table 1 may not display RyR1 activity, regardless of their predicted EC_{2x} values by the QSAR model. In general, the predicted EC_{2x} values shown in Table 1 for these potentially inactive congeners are high (from 1.5 to 6.5 μM), showing that the model does not inaccurately predict high activity for these substitution patterns. Of this suite of congeners, only PCBs 123, 126, and 157 have evidence of effectively complete experimental inactivity (i.e., measured EC_{2x} values >100 μM). For the remainder of untested congeners meeting this substitution pattern, the estimated EC_{2x} values in Table 1 can be used for conservative risk assessments until suitable test work is completed.

As discussed by Simon et al.[57] there is a need to develop alternate toxicity schemes for PCBs that complement the established aryl hydrocarbon receptor mediated toxic equivalence factor (AhR-TEF) framework that is anchored to the high toxicity of 2,3,7,8-tetrachlorodibenzo-p-dioxin (2,3,7,8-TeCDD). In their work, these authors put forward a conceptual framework for calculating the relative neurotoxicity equivalent (NEQ) scheme of PCB mixtures. The NEQ scheme of Simon et al.[57] used the limited experimental data sets of Kodavanti et al. for [^{3}H]phorbol ester binding,[13] Shain et al. for dopamine release from PC12 cells,[3] and Kodavanti et al. for microsomal and mitochondrial calcium release,[23] as well as the EC_{2x} and EC_{50} data from Pessah et al. for ryanodine binding.[42] However, and as noted by Simon et al. in their encouragement of extensions to their scheme,[57] approaches that use only experimental data for selected PCB congeners are highly vulnerable to possible selection bias in the experimental data sets. In other words, experimental data for each of these toxicological endpoints are only available for <10 to 20% of all possible PCB congeners. As a result, when attempting to extrapolate the limited experimental data set to provide insights on the relative toxicities of homologue groups and/or technical mixtures, the resulting interpretations may be subject to bias where the congeners tested are not representative (i.e., are significantly more or less toxic) than the remaining members of whatever categorization class they are placed in. Consequently, we also sought to complement and extend the NEQ scheme for RyR1 activity developed by Simon et al.[57] by incorporating the present QSAR development to estimate the desired toxicity of all PCB congeners. These EC_{2x} estimates can then be used to supplement the experimental data set for comprehensive full congener NEQ assessments. For our development of a full congener RyR1 activity NEQ scheme (RyR1-NEQ), we were unable to incorporate the EC_{50} data of Pessah et al.[42] given the poor quality optimized QSAR obtained from the experimental data set. Thus, the RyR1-NEQ scheme presented herein uses only the EC_{2x} data set. If future work finds a suitable QSAR for the EC_{50} data set, these findings can readily be integrated into our results.

Summaries of full congener ortho substitution pattern, homologue grouping, and Aroclor mixture RyR1-NEQs are given in Table 2. On a mass normalized basis, increasing ortho substitution increases the average RyR1 potency (tetra>tri>di>mono>non-ortho), as does increasing chlorination. However, we note that the observed effect of increasing RyR1-NEQs with increasing homologue number is an indirect reflection of the molecular controls on the toxicity. In other words, congeners with multiple ortho substituents are more likely to be found in higher homologues. For example, the percentage of congeners within a homologue with two or more ortho substituents are as follows: mono-CB, 0%; di-CB, 17%; tri-CB, 33%; tetra-CB, 55%; penta-CB, 72%; hexa-CB, 86%; hepta-CB, 96%; octa-CB, 100%; nona-CB, 100%; and deca-CB; 100%. Thus, favorable chlorination patterns for RyR1 potency are more likely to be found in the high homologue groupings. Similarly, increasing potency is predicted for the higher homologue Aroclor mixtures.

We also note that where all congeners in Table 1, plus PCB 75, are assumed to have RyR1-neurotoxicity equivalency factors (NEFs) of zero, there are only small corresponding changes in the homologue RyR1-NEQs that are well within the QSAR modelling errors. Since none of the congeners in Table 1, or PCB 75, is a significant component of any Aroclor technical mixture, there are no changes to Aroclor NEQs, whether either the QSAR RyR1-NEFs

Table 2. RyR1-NEQs for the full congener PCB ortho substitution groups, homologues, and major Aroclor technical mixtures (Aroclor compositions from ref. [57]).

Substitution pattern	*RyR1-NEQ (mg g^{-1} group)*
non-ortho	0.033 (0.030)
mono-ortho	0.077 (0.074)
di-ortho	0.154 (0.154)
tri-ortho	0.293 (0.293)
tetra-ortho	0.413 (0.413)
Homologue	*RyR1-NEQ (mg g^{-1} homologue)*
mono-CB	0.056 (0.056)
di-CB	0.056 (0.056)
tri-CB	0.078 (0.080)
tetra-CB	0.129 (0.136)
penta-CB	0.176 (0.187)
hexa-CB	0.220 (0.236)
hepta-CB	0.284 (0.293)
octa-CB	0.357 (0.357)
nona-CB	0.405 (0.405)
deca-CB	0.395 (0.395)
Technical mixture	*RyR1-NEQ (mg g^{-1} Aroclor)*
Aroclor 1016	0.080 (0.080)
Aroclor 1221	0.069 (0.069)
Aroclor 1232	0.069 (0.069)
Aroclor 1242	0.089 (0.089)
Aroclor 1248	0.122 (0.122)
Aroclor 1254	0.130 (0.130)
Aroclor 1260	0.197 (0.197)
Aroclor 1262	0.230 (0.230)
Aroclor 1268	0.323 (0.323)

Values in parentheses represent RyR1-NEQs where the RyR1-NEFs of all congeners in Table 1, as well as that of PCB 75, were assumed at zero.

or values of zero for these congeners are used. It is also important to stress that the possible synergistic and/or antagonistic effects of PCB mixtures are poorly defined,[22] but may confound efforts to develop a reliable and robust neurotoxicity equivalence scheme.

The potentially high RyR1 activity of various PCB metabolites will also complicate neurotoxicity risk assessments, as the differential rates of accumulation, metabolism, and excretion for both the PCB precursors, as well as the metabolites themselves, are poorly defined. Consequently, unless PCB exposure is at a continuous steady-state condition, the signatures of PCBs and their metabolites in vivo are continuously in flux, leading to difficulties in extrapolating the results of single-point analyses to a longer term risk perspective. Pessah et al.[42] showed that the hydroxy-PCB, 4-OH-PCB 136 ($pK_a = 6.25$), had relatively low RyR1 activity ($EC_{2x} = 1.60 \pm 0.26$ μM; EC_{50} = above solubility limit), as did 3′-OH-PCB 9 ($EC_{2x} = 1.69 \pm 0.14$ μM; $EC_{50} = 3.50 \pm 0.21$ μM; $pK_a = 9.74$) and 4′-OH-PCB 9 ($EC_{2x} = 1.38 \pm 0.12$ μM; $EC_{50} = 2.25 \pm 0.11$ μM; $pK_a = 9.49$), whereas 4′-OH-PCB 30 had high activity ($EC_{2x} = 0.32 \pm 0.04$ μM; $EC_{50} = 0.75 \pm 0.08$ μM; $pK_a = 9.43$).

By comparison, methyl sulfonyl and dihydroxy-PCB metabolites were effectively inactive. One difficulty in assessing the relative RyR1 potencies, or other toxicological endpoints, of hydroxy-PCBs is that the acidities of their phenolic groups are highly dependent on the degree and pattern of chlorine substitution. Thus, with a predicted pK_a of about 6.3, we would expect 4-OH-PCB 136 to be substantially dissociated in vivo, whereas 3′-OH-PCB 9, 4′-OH-PCB 9, and 4′-OH-PCB 30 (pK_a values >9.4) would primarily exist in vivo in their molecular forms. Thus, if ionization plays a major role in the RyR1 potency of a particular hydroxy-PCB congener (i.e., the EC_{2x} of the molecular and ionized form are significantly different), then QSARs developed for the parent PCBs will need to include ionization effects in an overall model beyond simple structural configurations of the chlorine substituents.

In addition, Pessah et al. have recently shown enantiomeric specificity of (−)-2,2′,3,3′,6,6′-PCB 136 towards both RyR1 and the corresponding type 2 ryanodine receptor (RyR2).[58] (−)-PCB 136 displayed an EC_{50} of about 0.95 μM towards both RyR1 and RyR2, whereas (+)–PCB 136 was inactive at concentrations <10 μM. An initial conclusion from this finding might be that for the 19 chiral PCB congeners (45, 84, 88, 91, 95, 131, 132, 135, 136, 139, 144, 149, 171, 174, 175, 176, 183, 196, and 197),[59] if one enantiomer is inevitably substantially weaker in RyR1 potency than the other, the racemic EC_{2x} values measured or estimated for these congeners should be divided in half to represent the EC_{2x} value of the most potent enantiomer (even if the identity of the enantiomer is not known). However, Lehmler et al. have reported that (−)-PCB 84 was only modestly more potent than (+)–PCB 84 at increasing [^{3}H]-phorobol ester binding, and that no enantiomeric specificity existed towards the inhibition of $^{45}Ca^{2+}$ uptake.[60]

Consequently, in the absence of additional data, it is unclear whether, as Pessah et al.[58] have stated, the degree of RyR1 enantioselectivity may be different among various chiral PCBs. Furthermore, this group has also reported more pronounced effects of PCB 95 on [^{3}H]Ry receptor binding to $_{MH}$RyR1 (from pigs homozygous for the malignant hyperthermia mutation) than $_{Wt}$RyR1 (from wild type pigs),[34] suggesting that individuals possessing malignant hyperthermia mutations within RyR1 may be more susceptible to adverse effects from non-coplanar PCB exposure. As with the potential enantioselective nature of chiral PCBs towards RyR1, at this point, the lack of a multicongener data set for establishing differential potencies of PCBs towards $_{MH}$RyR1 and $_{Wt}$RyR1 prevents inclusion of this additional information in any current QSAR models.

Conclusions

A quantitative structure-activity relationship (QSAR) was developed to predict the congener specific ryanodine receptor type RyR1 activity for the 209 polychlorinated biphenyl

(PCB) congeners. A three-variable QSAR equation with a high quality of fit was obtained via stepwise forward linear regression on an unsupervised forward selection reduced data set from an initial database of about 1700 molecular descriptors with a 29 congener training set containing experimental PCB congener concentrations required to enhance specific [^{3}H]RyR1 binding by two-fold (EC_{2x}). Good agreement in substitution pattern trends was obtained between the experimental and estimated data sets. The QSAR predicts PCBs 94, 135, 152, 178, 179, 200, 201, 202, 208, and 209 will have RyR1 activation potencies equal to, or exceeding, the most potent congeners in the experimental data set, suggesting these congeners should be included in future experimental studies.

However, no PCB congeners are predicted to have EC_{2x} values much less than 0.2 μM, suggesting the limited experimental data reported to date appears to have adequately mapped the range of potential PCB RyR1 activities. Integration of the experimental and estimated EC_{2x} values into a mass normalized full congener RyR1 activity neurotoxicity equivalence (RyR1-NEQ) scheme indicates that increasing ortho substitution increases the average RyR1 potency (tetra>tri>di>mono>non-ortho), as does increasing chlorination on both a homologue and Aroclor mixture basis. However, increasing RyR1-NEQs with increasing homologue number and Aroclor chlorination likely reflect indirect molecular controls on toxicity, rather than a hydrophobicity control, since congeners with multiple ortho substituents are more likely to be found in higher homologues.

References

[1] Hansen, L.G. Stepping backward to improve assessment of PCB congener toxicities. Environ. Health Perspect. **1998**, *106*, 171–189.

[2] Seegal, R.F.; Bush, B.; Shain, W. Neurotoxicology of ortho-substituted polychlorinated biphenyls. Chemosphere **1991**, *23*, 1941–1949.

[3] Shain, W.; Bush, B.; Seegal, R. Neurotoxicity of polychlorinated biphenyls: Structure-activity relationship of individual congeners. Toxicol. Appl. Pharmacol. **1991**, *111*, 33–42.

[4] Seegal, R.F. Epidemiological and laboratory evidence of PCB-induced neurotoxicity. Crit. Rev. Toxicol. **1996**, *26*, 709–737.

[5] Fischer, L.J.; Seegal, R.F.; Ganey, P.E.; Pessah, I.N.; Kodavanti, P.R. Symposium overview: Toxicity of non-coplanar PCBs. Toxicol. Sci. **1998**, *41*, 49–61.

[6] Inglefield, J.R.; Mundy, W.R.; Shafer, T.J. Inositol 1,4,5-triphosphate receptor-sensitive $Ca^{(2+)}$ release, store-operated $Ca^{(2+)}$ entry, and cAMP responsive element binding protein phosphorylation in developing cortical cells following exposure to polychlorinated biphenyls. J. Pharmacol. Exp. Ther. **2001**, *297*, 762–773.

[7] Inglefield, J.R.; Shafer, T.J. Polychlorinated biphenyl-stimulation of $Ca^{(2+)}$ oscillations in developing neocortical cells; A role for excitatory transmitters and L-type voltage-sensitive $Ca^{(2+)}$ channels. J. Pharmacol. Exp. Ther. **2000**, *295*, 105–113.

[8] Mundy, W.R.; Shafer, T.J.; Tilson, H.A.; Kodavanti, P.R. Extracellular calcium is required for the polychlorinated biphenyl-induced increase of intracellular free calcium levels in cerebellar granule cell culture. Toxicology **1999**, *136*, 27–39.

[9] Schantz, S.L.; Seo, B.W.; Wong, P.W.; Pessah, I.N. Long-term effects of developmental exposure to 2,2′,3,5′,6-pentachlorobiphenyl (PCB 95) on locomotor activity, spatial learning and memory and brain ryanodine binding. Neurotoxicology **1997**, *18*, 457–467.

[10] Safe, S.H. Polychlorinated biphenyls (PCBs): Environmental impact, biochemical and toxic responses, and implications for risk assessment. Crit. Rev. Toxicol. **1994**, *24*, 87–149.

[11] Seegal, R.F.; Brosch, K.O.; Bush, B. Polychlorinated biphenyls produce regional alterations of dopamine metabolism in rat brain. Toxicol. Lett. **1986**, *30*, 197–202.

[12] Seegal, R.F.; Bush, B.; Brosch, K.O. Sub-chronic exposure of the rat to Aroclor 1254 selectively alters central dopaminergic function. NeuroToxicology **1991**, *12*, 55–66.

[13] Kodavanti, P.R.; Ward, T.R.; McKinney, J.D.; Tilson, H.A. Increased [^{3}H]phorbol ester binding in rat cerebellar granule cells by polychlorinated biphenyl mixtures and congeners: Structure-activity relationships. Toxicol. Appl. Pharmacol. **1995**, *130*, 140–148.

[14] Seegal, R.F.; Bush, B.; Brosch, K.O. Comparison of effects of Aroclors 1016 and 1260 on non-human primate catecholamine function. Toxicology **1991**, *66*, 145–163.

[15] Seegal, R.F.; Bush, B.; Brosch, K.O. Decreases in dopamine concentrations in adult, nonhuman primate brain persist following removal from polychlorinate biphenyls. Toxicology **1994**, *86*, 71–87.

[16] Seegal, R.F.; Bush, B.; Shain, W. Lightly chlorinated ortho-substituted PCB congeners decrease dopamine in nonhuman primate brain and in tissue culture. Toxicol. Appl. Pharmacol. **1990**, *106*, 136–144.

[17] Seegal, R.F.; Bush, B.; Shain, W. PCB neurotoxicity is associated with non-planar ortho-substituted congeners. Toxicologist **1990**, *10*, 252.

[18] Kodavanti, P.R.S.; Shin, D.; Tilson, H.A.; Harry, G.J. Comparative effects of two polychlorinated biphenyl congeners on Ca^{2+}-homeostasis in rat cerebellar granule cells. Toxicol. Appl. Pharmacol. **1993**, *123*, 97–106.

[19] Kodavanti, P.R.; Shafer, T.J.; Ward, T.R.; Mundy, W.R.; Freudenrich, T.; Harry, G.J.; Tilson, H.A. Differential effects of polychlorinated biphenyl congeners on phosphoinositide hydrolysis and protein kinase C translocation in rat cerebellar granule cells. Brain Res. **1994**, *662*, 75–82.

[20] Kodavanti, P.R.; Ward, T.R.; McKinney, J.D.; Waller, C.L.; Tilson, H.A. Increased [^{3}H] phorbolester binding in rat cerebellar granule cells and inhibition of $^{45}Ca^{2+}$ sequestration in rat, cerebellum by polychlorinated diphenyl ether congeners and analogs: Structure–activity relationships. Toxicol. Appl. Pharmacol. **1996**, *138*, 251–261.

[21] Kodavanti, P.R.; Tilson, H.A. Structure-activity relationships of potentially neurotoxic PCB congeners in the rat. Neurotoxicology **1997**, *18*, 425–441.

[22] Kodavanti, P.R.; Tilson, H.A. Comments on "Developmental neurotoxicity of PCBs in humans: What do we know and where do we go from here?". Neurotoxicol. Teratol. **1997**, *19*, 1–5.

[23] Kodavanti, P.R.; Ward, T.R.; McKinney, J.D.; Tilson, H.A. Inhibition of microsomal and mitochondrial Ca^{2+}-sequestration in rat cerebellum by polychlorinated biphenyl mixtures and congeners. Structure-activity relationships. Arch. Toxicol. **1996**, *70*, 150–157.

[24] Kodavanti, P.R.; Ward, T.R.; Ludewig, G.; Robertson, L.W. Birnbaum, L.S. Polybrominated diphenyl ether (PBDE) effects in rat neuronal cultures: 14C–PBDE accumulation, biological effects, and structure–activity relationships. Toxicol. Sci. **2005**, *88*, 181–192.

[25] Kodavanti, P.R.S.; Ward, T.R. Differential effects of commercial polybrominated diphenyl ether and polychlorinated biphenyl mixtures on intracellular signaling in rat brain in vitro. Toxicol. Sci. **2005**, *85*, 952–962.

[26] Kodavanti, P.R.S.; Ward, T.R.; Derr-Yellin, E.C.; McKinney, J.D.; Tilson, H.A. Increased [^{3}H]phorbol ester binding in rat cerebellar granule cells and inhibition of ^{45}Ca *(2+)* buffering in rat cerebellum by hydroxylated polychlorinated biphenyls. Neurotoxicology **2003**, *24*, 187–198.

[27] Howard, A.S.; Fitzpatrick, R.; Pessah, I.; Kostyniak, P.; Lein, P.J. Polychlorinated biphenyls induce caspase-dependent cell death in cultured embryonic rat hippocampal but not cortical neurons via activation of the ryanodine receptor. Toxicol. Appl. Pharmacol. **2003**, *190*, 72–86.

[28] Wong, P.W.; Pessah, I.N. Ortho-substituted polychlorinated biphenyls alter calcium regulation by a ryanodine receptor-mediated mechanism: Structural specificity toward skeletal- and cardiac-type microsomal calcium release channels. Mol. Pharmacol. **1996**, *49*, 740–751.

[29] Wong, P.W.; Brackney, W.R.; Pessah, I.N. Ortho-substituted polychlorinated biphenyls alter microsomal calcium transport by direct interaction with ryanodine receptors of mammalian brain. J. Biol. Chem. **1997**, *272*, 15145–15153.

[30] Wong, P.W.; Joy, R.M.; Albertson, T.E.; Schantz, S.L.; Pessah, I.N. Ortho-substituted 2,2′,3,5′,6-pentachlorobiphenyl (PCB 95) alters rat hippocampal ryanodine receptors and neuroplasticity in vitro: Evidence for altered hippocampal function. Neurotoxicology **1997**, *18*, 443–456.

[31] Wong, P.W.; Pessah, I.N. Noncoplaner PCB 95 alters microsomal calcium transport by an immunophilin FKBP12–dependent mechanism. Mol. Pharmacol. **1997**, *51*, 693–702.

[32] Wong, P.W.; Garcia, E.F.; Pessah, I.N. Ortho-substituted PCB95 alters intracellular calcium signaling and causes cellular acidification in PC12 cells by an immunophilin-dependent mechanism. J. Neurochem. **2001**, *76*, 450–463.

[33] Gafni, J.; Wong, P.W.; Pessah, I.N. Non-coplanar 2,2′,3,5′,6-pentachlorobiphenyl (PCB 95) amplifies ionotropic glutamate receptor signaling in embryonic cerebellar granule neurons by a mechanism involving ryanodine receptors. Toxicol. Sci. **2004**, *77*, 72–82.

[34] Ta, T.A.; Pessah, I.N. Ryanodine receptor type 1 (RyR1) possessing malignant hyperthermia mutation R615C exhibits heightened sensitivity to dysregulation by non-coplanar 2,2′,3,5′,6-pentachlorobiphenyl (PCB 95). Neurotoxicology **2007**, *28*, 770–779.

[35] Giannini, G.; Conti, A.; Mammarella, S.; Scrobogna, M.; Sorrentino, V. The ryanodine receptor/calcium channel genes are widely and differentially expressed in murine brain and peripheral tissues. J. Cell Biol. **1995**, *128*, 893–904.

[36] Hakamata, Y.; Nakai, J.; Takeshima, H.; Imoto, K. Primary structure and distribution of a novel ryanodine receptor/calcium release channel from rabbit brain. FEBS Lett. **1992**, *312*, 229–235.

[37] Marks, A.R.; Tempst, P.; Hwang, K.S.; Taubman, M.B.; Inui, M.; Chadwick, C.; Fleischer, S.; Nadal-Ginard, B. Molecular cloning and characterization of the ryanodine receptor/junctional channel complex cDNA from skeletal muscle sarcoplasmic reticulum. Proc. Natl. Acad. Sci. **1989**, *86*, 8683–8687.

[38] Nakai, J.; Imagawa, T.; Hakamat, Y.; Shigekawa, M.; Takeshima, H.; Numa, S. Primary structure and functional expression from cDNA of the cardiac ryanodine receptor/calcium release channel. FEBS Lett. **1990**, *271*, 169–177.

[39] Takeshima, H.; Nishimura, S.; Matsumoto, T.; Ishida, H.; Kangawa, K.; Minamino, N.; Matsuo, H.; Ueda, M.; Hanaoka, M.; Hirose, T. Primary structure and expression from complementary DNA of skeletal muscle ryanodine receptor. Nature **1989**, *339*, 439–445.

[40] Crofton, K.M.; Kodavanti, P.R.; Derr-Yellin, E.C.; Casey, A.C.; Kehn, L.S. PCBs, thyroid hormones, and ototoxicity in rats: Cross-fostering experiments demonstrate the impact of postnatal lactation exposure. Toxicol. Sci. **2000**, *57*, 131–140.

[41] Van Oostdam, J.C.; Dewailly, E.; Gilman, A.; Hansen, J.C.; Odland, J.O.; Chashchin, V.; Berner, J.; Butler-Walker, J.; Lagerkvist, B.J.; Olafsdottir, K.; Soininen, L.; Bjerregard, P.; Klopov, V.; Weber, J.P. Circumpolar maternal blood contaminant survey, 1994–1997 organochlorine compounds. Sci. Total Environ. **2004**, *330*, 55–70.

[42] Pessah, I.N.; Hansen, L.G.; Albertson, T.E.; Garner, C.E.; Ta, T.A.; Do, Z.; Kim, K.H.; Wong, P.W. Structure-activity relationship for noncoplanar polychlorinated biphenyl congeners toward the ryanodine receptor-Ca^{2+} channel complex type 1 (RyR1). Chem. Res. Toxicol. **2006**, *19*, 92–101.

[43] Weininger, D. SMILES: A chemical language and information system. 1. Introduction to methodology and encoding rules. J. Chem. Inf. Comp. Sci. **1988**, *28*, 31–36.

[44] Weininger, D.; Weininger, A.; Weininger, J.L. SMILES. 2. Algorithm for generation of unique SMILES notation. J. Chem. Inf. Comp. Sci. **1989**, *29*, 97–101.

[45] Tetko, I.V. Computing chemistry on the web. Drug Discov. Today **2005**, *10*, 1497–1500.

[46] Tetko, I.V.; Gasteiger, J.; Todeschini, R.; Mauri, A.; Livingstone, D.; Ertl, P.; Palyulin, V.A.; Radchenko, E.V.; Zefirov, N.S.; Makarenko, A.S.; Tanchuk, V.Y.; Prokopenko, V.V. Virtual computational chemistry laboratory: Design and description. J. Comput. Aided Mol. Des. **2005**, *19*, 453–463.

[47] Hilal, S.; Karickhoff, S.; Carreira, L. Prediction of the solubility, activity coefficient and liquid/liquid partition coefficient of organic compounds. QSAR Comb. Sci. **2004**, *23*, 709–720.

[48] Hilal, S.H.; Karickhoff, S.W.; Carreira, L.A. A rigorous test for SPARC's chemical reactivity models: Estimation of more than 4300 ionization pK_as. Quant. Struc. Act. Relat. **1995**, *14*, 348–355.

[49] Allinger, N.L. Conformational analysis. 130. MM2. A hydrocarbon force field utilizing V1 and V2 torsional terms. J. Am. Chem. Soc. **1977**, *99*, 8127–8134.

[50] Klamt, A.; Schourmann, G. COSMO: A new approach to dielectric screening in solvents with explicit expressions for the screening energy and its gradient. J. Chem. Soc., Perkin Trans. 2 **1993**, 799–805.

[51] Stewart, J. Optimization of parameters for semiempirical methods V: Modification of NDDO approximations and application to 70 elements. J. Molec. Model. **2007**, *13*, 1173–1213.

[52] Whitley, D.C.; Ford, M.G.; Livingstone, D.J. Unsupervised forward selection: A method for eliminating redundant variables. J. Chem. Inf. Comput. Sci. **2000**, *40*, 1160–1168.

[53] Taraviras, S.L.; Ivanciuc, O.; Cabrol-Bass, D. Identification of groupings of graph theoretical molecular descriptors using a hybrid cluster analysis approach. J. Chem. Inf. Comput. Sci. **2000**, *40*, 1128–1146.

[54] Bendel, R.B.; Afifi, A.A. Comparison of stopping rule in forward stepwise regression. J. Amer. Statist. Assoc. **1977**, *72*, 46–53.

[55] Wei, D.; Zhang, A.; Wu, C.; Han, S.; Wang, L. Progressive study and robustness test of QSAR model based on quantum chemical parameters for predicting BCF of selected polychlorinated organic compounds (PCOCs). Chemosphere **2001**, *44*, 1421–1428.

[56] Dogra, S.K. Cross-validation. QSARWorld—A Strand Life Sciences Web Resource **2009**, *http://www.qsarworld.com/qsar-ml-cross-validation.php*, (accessed 20 May 2009).

[57] Simon, T.; Britt, J.K.; James, R.C. Development of a neurotoxic equivalence scheme of relative potency for assessing the risk of PCB mixtures. Regul. Toxicol. Pharmacol. **2007**, *48*, 148–170.

[58] Pessah, I.N.; Lehmler, H.; Robertson, L.W.; Perez, C.F.; Cabrales, E.; Bose, D.D.; Feng, W. Enantiomeric specificity of (-)-2,2′,3,3′,6,6′-hexachlorobiphenyl toward ryanodine receptor types 1 and 2. Chem. Res. Toxicol. **2009**, *22*, 201–207.

[59] Kaiser, K.L.E. On the optical activity of polychlorinated biphenyls. Environ. Poll. **1974**, *7*, 93–101.

[60] Lehmler, H.; Robertson, L.W.; Garrison, A.W.; Kodavanti, P.R.S. Effects of PCB 84 enantiomers on [^{3}H]-phorbol ester binding in rat cerebellar granule cells and $^{45}Ca^{2+}$-uptake in rat cerebellum. Toxicol. Lett. **2005**, *156*, 391–400.